

Optical absorption and luminescence of α - LiV_2O_5 from the Bethe Salpeter Equation

Claudio Garcia and Walter R. L. Lambrecht*

*Department of Physics, Case Western Reserve University,
10900 Euclid Avenue, Cleveland, OH-44106-7079, USA*

α - $\text{Li}_x\text{V}_2\text{O}_5$ is obtained by intercalating Li between the layers of V_2O_5 . The partial filling of the split-off conduction band by electron donation from Li leads to significant changes in optical properties. Here we study the electronic band structure of α - LiV_2O_5 using quasiparticle self-consistent (QS) GW calculations and the optical dielectric function by means of the Bethe Salpeter equation. We find a very strong optical absorption band related to transitions between the filled $V-d_{xy}$ like states to the empty ones with strong polarization along the a -direction. We relate this to recent experimental observations of cathodoluminescence (CL) in which a suppression of the CL was observed upon addition of Li.

I. INTRODUCTION

Vanadium pentoxide or V_2O_5 is a layered oxide with strongly anisotropic properties in the layers thanks to the 1D zigzag chains of edge connected alternatingly up and down pointing square pyramids surrounding each V.[1] Its properties can be significantly tuned by intercalating with Li, Na, Mg and other ions. These atoms are located in between the van der Waals bonded layers in the

large open channels between the double zigzag chains, which are connected via a bridge oxygen. See Fig. 1 for the crystal structure. These ions can thus easily diffuse in and out of the structure and this provides a way to tune the properties of the material forming so-called V_2O_5 bronzes. This makes $\text{Li}_x\text{V}_2\text{O}_5$ attractive as a Li cathode material, since up to a certain concentration, the Li insertion and removal is reversible without significant structural changes. The study of V_2O_5 as a host for Li cathode battery material goes back to the work of the chemistry Nobel Prize winner Stanley Wittingham [2, 3] and has recently been re-activated by various authors.[4–11] Optical characterization can play an important role in elucidating the electrochemical insertion and extraction of Li.

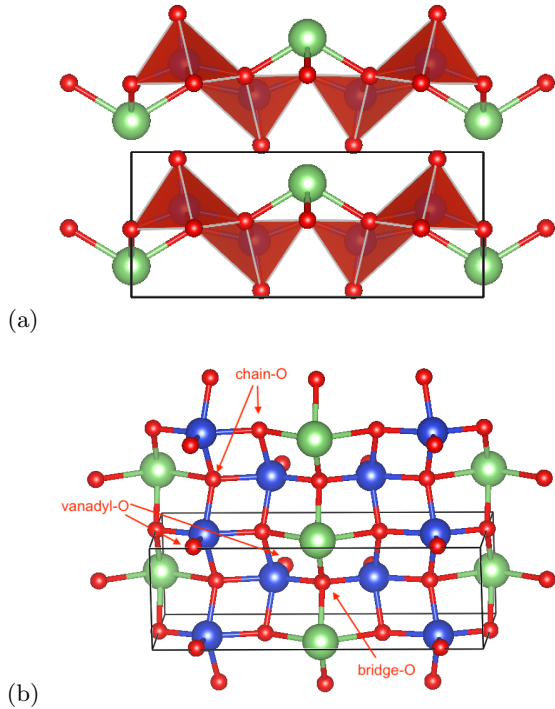


Fig. 1: Structure of α - LiV_2O_5 : (a) side view with V-surrounding polyhedra and (b) top view (ball and stick): green spheres Li, blue sphere V, red spheres O.

Walker *et al.* [4] used depth resolved Cathodoluminescence (CL) to study the evolution of the CL signal as function of Li uptake and the accompanying changes in the structure of $\text{Li}_x\text{V}_2\text{O}_5$ were also studied by Raman spectroscopy by Jarry *et al.* [5]. The modifications of the optical properties observed in this work can be utilized for electrochromic applications as they modify the color of the crystals. Walker *et al.* [4] observed a decrease in the lowest energy CL peak (1.8-1.9 eV) upon Li uptake which they analyzed in terms of local density approximation (LDA) band structure calculations by Eyert and Höck [12] and recent X-ray edge spectroscopy studies of $\text{Li}_x\text{V}_2\text{O}_5$ [13, 14]. However, it has recently become clear that the optical properties of V_2O_5 are not well described by a simple interband transition picture based on band structure theory. Quasiparticle self-consistent GW calculations by Bhandari *et al.* [15] showed that the quasiparticle gap is much larger (~ 4.4 eV) than the optical absorption edge of 2.3 eV extracted from Tauc-plots by Kenny and Kannewurf[16]. Recently, this discrepancy was resolved by pointing out the large excitonic binding energies in this material[17, 18]. The interpretation of the optical properties of $\text{Li}_x\text{V}_2\text{O}_5$ thus requires revision in terms of our current understanding of the excitonic properties of V_2O_5 . Polaronic effects are also known to play an important role in V_2O_5 . Since early work on the transport it is known that the electronic transport

* walter.lambrecht@case.edu

is essentially of the variable range hopping type associated with small polarons.[19] The strong electron-phonon coupling in V_2O_5 was shown to lead to self-trapped polarons by Scanlon *et al.* [20] and later further studied by Ngamwongwan *et al.* [21] and Wathaisong *et al.* [22].

In this paper we calculate the electronic structure of LiV_2O_5 using the QSGW method[23] and evaluate the optical absorption properties using the recent implementation [24, 25] of the Bethe Salpeter Equation approach based on the linearized-muffin-tin-orbital (LMTO) basis set [26].

First, we note that for one Li per V_2O_5 unit the lowest split-off conduction band becomes exactly half-filled and this leads to the formation of a magnetic moment and a spin-polarized band structure. In analogy with NaV_2O_5 , we expect the spins to be ordered antiferromagnetically along the chains[27]. While the ordering of spins in LiV_2O_5 requires further study we here adopt this same spin arrangement and study the optical properties in both ferromagnetic (FM) and antiferromagnetic (AFM) LiV_2O_5 . It is known from various studies of the lithiation [10, 11, 28] that upon higher concentration of Li, a phase transition occurs to first the γ -phase of LiV_2O_5 , which can already accommodate more than one Li per V_2O_5 unit. For $Li_2V_2O_5$, the split-off band would become completely filled and magnetic moment formation is then no longer evident. At even higher concentration $Li_3V_2O_5$ a non-layered (disordered rocksalt-type) ω -structure has been obtained [10, 11, 28, 29] In the present paper we only consider the regime where the structure stays close to that of α - V_2O_5 , *i.e.* $x \leq 1$ although even there small modifications occur and have been labeled as the ϵ - and δ -phases.

Our primary goal is to provide an alternative interpretation for the CL key observation of a reduction of the lowest CL peak at about 1.8 eV upon the initial lithiation.

II. COMPUTATIONAL METHODS

The band structures are calculated using the QSGW method [30], for which details of the implementation are given in [23]. This is a variant of Hedin's GW method in which G is the one-electron Green's function and W the screened Coulomb interaction [31, 32] and determine the dynamic self-energy $\Sigma = iGW$. In the quasiparticle self-consistent approach, a non-local but energy independent exchange correlation potential $\tilde{\Sigma} = \frac{1}{2} \sum_{ij} |\psi_i\rangle \Re\{\Sigma_{ij}(\epsilon_i) + \Sigma_{ij}(\epsilon_j)\} \langle\psi_j|$ is extracted from the energy-dependent self-energy $\Sigma(\omega)$, with $|\psi_i\rangle$ the eigenstates of the non-interacting Hamiltonian H_0 and \Re meaning the Hermitian part. This allows to iteratively update and thereby optimize the H_0 starting from a density functional theory (DFT) functional such as LDA or generalised gradient approximation (GGA) and makes the final results independent of the starting exchange-correlation functional choice. It focuses on the quasi-

particle energies rather than the full self-energy or interacting one-electron Green's function and this approach was further justified by Ismail-Beigi[33]. The QUESTAAL code implementation of this method used here uses a muffin-tin-orbital basis set and is described in [26]. For the two-point quantities like the bare v and screened $W = \epsilon^{-1}v = (1-vP)^{-1}v$ Coulomb potentials and the polarization P and inverse dielectric function ϵ^{-1} it uses a mixed-product basis set, including plane waves restricted to the interstitial region and products of partial waves times spherical harmonics in the muffin-tin spheres. This idea originates from [34] and provides an efficient way to describe the screening at short range which does not require high energy partial waves or high energy conduction bands. More recently, the Bethe Salpeter Equation (BSE) method [35] which uses the two-particle Green's function to study the optical properties including local field and electron-hole interaction effects, was also implemented in the QUESTAAL code package and an improvement beyond the random phase approximation (RPA) for the screening of the W is also based on the BSE was implemented and described in [24, 25]. Details of the present calculation are similar to our recent study of optical properties in V_2O_5 [18]. The convergence parameters were carefully optimized. We use a double set of smoothed Hankel function envelope functions with optimized decay lengths κ and associated smoothing radii with angular momenta $spdfsp$ for V and O and $spdsp$ for Li and include V-3p semi-core states as local orbitals. We use a $1 \times 5 \times 5$ \mathbf{k} -point mesh and a cut-off of the self-energy of 2.13 Rydberg above which it is approximated by an average diagonal value. We start the QSGW calculations with a GGA+ U calculation, using the Perdew-Burke-Ernzerhof (PBE) [36] functional with a Hubbard U of 0.1 Rydberg on the V- d orbitals to initiate a magnetic moment, but which is then switched off as the GW self-energy takes over the role of the Hubbard U . The results thus do not depend on this initial choice, which is only used to start from a band structure with a spin-splitting due to the half-filling of the narrow split-off conduction band.

Unlike our previous study on V_2O_5 which used the QSGW method in which electron-hole interaction effects are included in the screening of W , we here use the original QSGW method. While this increases the gaps (indirect, lowest direct and direct at Γ) of V_2O_5 by about 0.6 eV compared to the more accurate \hat{W} approach, the exciton binding energies are then also larger and the energy of the lowest optical excitations are only overestimated by ~ 0.4 eV. We are here focusing on qualitative changes due to Li and avoided the more time consuming BSE evaluation of screened \hat{W} .

III. RESULTS

We start by comparing the QSGW band structure results for pure V_2O_5 with those of FM LiV_2O_5 shown in

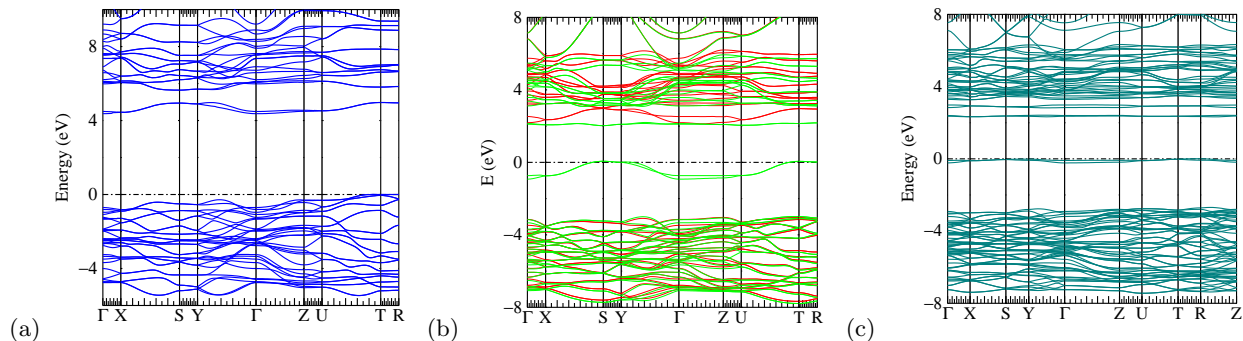


Fig. 2: QSGW band structures of (a) V_2O_5 , (b) FM LiV_2O_5 , (c) AFM LiV_2O_5 ; blue non-spinpolarized, green majority, red minority spin; orange up and down spin superposed

Fig. 2a-b. As already announced in the introduction, we can see that the narrow split-off conduction band at about 4 eV above the VBM, splits in spin-up and spin-down bands, the lower of which is then occupied by the extra electron donated by the Li. The exchange splitting of this band is about 2.9 eV. The splitting between the two lowest majority spin conduction bands is about 2.8 eV at Γ and 2.1 at Y , where it is lowest. In pure V_2O_5 at Γ , the split-off band lies about 1.5 eV below the bottom of the main set of conduction bands while this splitting is lower at Y , where it is about 0.8 eV in V_2O_5 . So, this makes sense: at its maximum near Y , the split-off band in V_2O_5 is about 0.8 eV below the main CBM and the spin-splitting induced in LiV_2O_5 then places the majority spin 1.4 eV below this point, so at about 2.2 eV below the main CBM or majority spin. We may also notice that the highest valence band which in pure V_2O_5 shows a significant dispersion along ΓZ becomes flatter in LiV_2O_5 . This indicates that the insertion of Li disrupts the interlayer hopping of the O-2p like states. The split-off band of majority spin has a band dispersion mostly along the ΓY direction, which is the b -direction along the chains and has a band width or about 0.8 eV. In FM LiV_2O_5 at Γ the bottom of the split-off band lies about 2.2 eV above the rather flat VBM of the O-2p bands. The gap at Γ from the O-2p like VBM to the majority spin CBM at Γ is 5.26 eV, which is slightly larger than in pure V_2O_5 where it is 5.07 eV. In a simple band-to-band transition picture, we may now expect new optical transitions between the occupied majority spin band at the lowest empty band of the same spin, at about 2 eV. Next, we can see that in AFM LiV_2O_5 , the situation is essentially the same but now the spin-up and spin-down bands are exactly superposed. Note that the spin-up bands on one V-O-V rung become the spin-down bands on the next rung along the b -direction and vice versa. Because of the doubling of the cell along b , the bands are folded. We may note that the highest occupied V- d_{xy} derived bands become almost dispersionless but the lowest gap is similar.

In terms of magnetic properties, we note that the net magnetic moment of the FM cell is $2 \mu_B$. Since there

are four V per cell, this means effectively $0.5 \mu_B$ per V. Indeed, because there are two formula units per unit cell, there are two bands of majority spin that become exactly filled while their spin-down counterpart stays empty. It indicates that we rather should consider the magnetic moment as being associated with a single V-O-V rung and equally spread over the two V in that rung. This makes sense as the lower split-off band is essentially a molecular type state formed by V- d_{xy} orbitals which is odd versus the mirror plane perpendicular to the a -crystallographic axis. As such it cannot interact with the O- p_y states of the bridge oxygen between them, while the higher conduction band at the bottom of the main conduction band manifold is an even combination of the same orbitals which does feel the antibonding π -type interaction with the O- p_y of the bridge. The O- p_x and p_z are orthogonal to the xy orbitals of the two V along the $a = x$ direction and do not come into play. The total energy can at present not reliably be calculated within the QSGW method. This would require a trace over all states, including very high-lying empty states via the Luttinger-Ward formula. Linear response function calculations indicate that the coupling between spins is antiferromagnetic along the b -direction, and this agrees with known experimental data in the related NaV_2O_5 . We reserve a discussion of the magnetic properties to a separate paper. We may then also assume that even in the paramagnetic case, locally magnetic moments form but are disordered and the electronic structure locally is similar to the one we here obtain for the FM case.

Next, we consider the optical properties calculated in BSE and the independent particle approximation (IPA) in Fig. 3. We show the results for both BSE (solid lines) and IPA (dashed lines) for $\mathbf{E} \parallel \mathbf{a}$ (black, blue) and $\mathbf{E} \parallel \mathbf{b}$ (red, green). In blue and green are the results using a converged set of 64 valence and 40 conduction bands, *i.e.* including all O-2p and V-3d derived bands, while in black and red we have used only 32 valence and 20 conduction bands. This shows that convergence in the number of bands is important. We do not include the $\mathbf{E} \parallel \mathbf{c}$ spectra as this is less relevant being polarized perpendicular to the layers and therefore difficult to measure

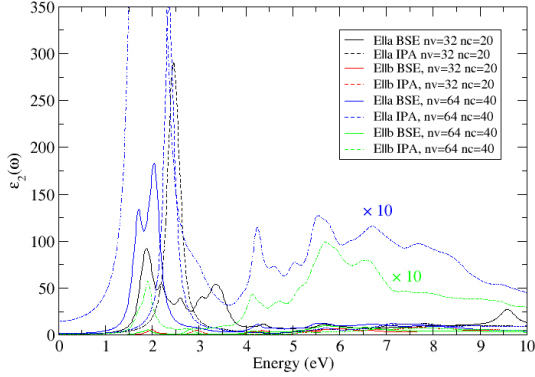


Fig. 3: Imaginary part of the dielectric function for AFM LiV_2O_5 .

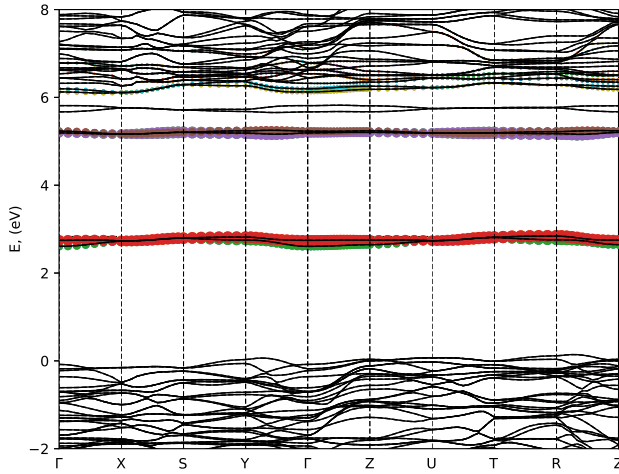


Fig. 4: Band weights contributions to the peak in $\varepsilon_2(\omega)$ in the range 1.7-1.85 eV.

experimentally. Compared to pure V_2O_5 , [17, 18] where the absorption starts with excitons at about 3.0 eV, the most notable is a new strong absorption band near 2 eV, polarized almost exclusively along a . To better see the converged BSE results in the energy region above ~ 4 eV we also show these curves multiplied by a factor 10 in dash-dotted lines and corresponding colors. The new absorption band is already present in the IPA as a narrow peak at 2.45 eV but shifts to 1.85 eV in BSE. At the same time, the charge transfer exciton related to the $\text{O}-2p$ to $\text{V}-3d_{xy}$ transitions also present in pure V_2O_5 at about 3 eV also shows up in BSE for both polarizations and the onset of band-to-band continuum lies at above 4 eV, corresponding to the quasiparticle gap.

The main new feature peaking at 1.85 eV corresponds to the transitions between the occupied split-

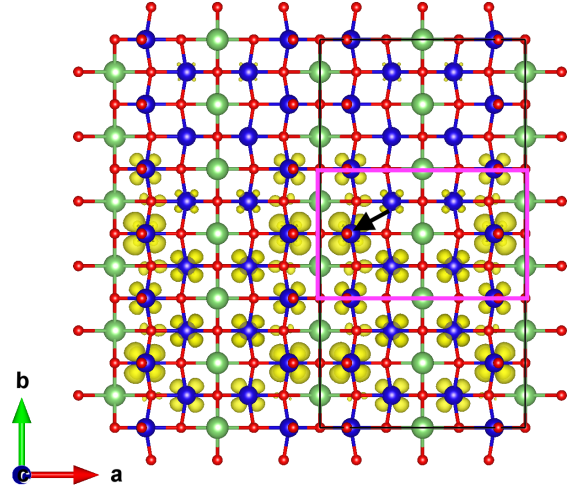


Fig. 5: Probability density of holes for electron paged on the V indicated by the arrow, for excitonic states in the range 1.7-1.9 eV.

off band to the lowest unoccupied conduction band, as can be seen in Fig. 4. This feature is similar to what was pointed out in NaV_2O_5 in Bhandari *et al.* [27] and was in that material also studied by electron loss spectroscopy[37]. In NaV_2O_5 , experimentally it lies at about 1 eV rather than near 2 eV. However, the QSGW gap between these states is also near 2 eV similar to the situation in LiV_2O_5 . Thus, strong excitonic effects again influence this optical transition as we can see by comparing BSE with IPA. Closer inspection of the excitonic eigenvalues, shows that there are also nearly dark excitons starting at about 1.4 eV.

A minor difference may result between Na and Li from the difference in distortion of the structure. The angle between the $\text{O}_b\text{-V-O}_v$ gives a measure of the tilting of the pyramid with its O_v towards the inserted alkali cation and is 102° for Li and 104° for Na. The sharper angle means more tilting. The distance from the vanadyl O_v toward the Na is 2.707 Å while toward the Li is 2.66 Å. These stronger distortions are consistent with a slightly stronger downward shift of the occupied $\text{V}-d_{xy}$ like state by interacting with the intercalated cation.

The reason this absorption is polarized exclusively along a is that it corresponds to transitions between odd and even states with respect to the mirror-plane passing through the bridge O and perpendicular to the a direction as was pointed out above. Since this is a transition between the molecular localized type states centered on the bridge O and having mainly $\text{V}-d_{xy}$ character for both states, is it mainly an intra-atomic transition and thereby significantly stronger than the charge-transfer type transitions. This can be seen in Fig.5. We can clearly see the xy character of the states. The strongest hole contribution is on the V where the electron is placed and its neighbor across the V-O-V rung.

IV. DISCUSSION OF THE CATHODOLUMINESCENCE

Walker *et al*[4] studied changes in the electronic structure of $\text{Li}_x\text{V}_2\text{O}_5$ using depth resolved CL. Each of their peaks shows considerable fine structure that evolves with depth from bulk to surface and is also shown to be sensitive to remote oxygen plasma treatment, indicating that O-vacancies play a role. It is here not our intent to interpret these fine changes but rather to understand the broad main features and their changes between pure V_2O_5 and LiV_2O_5 . Their spectrum for pure V_2O_5 shows a first peak just below 2 eV with fine structure at 1.8 and 1.9 eV, followed by a smaller peak near 3 eV and merging peaks at 3.6 and 4.1 eV. The main change upon lithiation is that the feature near 2 eV is strongly suppressed and essentially absent but can be partially restored by delithiation. These authors interpreted the feature near 2 eV as resulting from recombination of $V-d_{xy}$ like split-off conduction electrons recombining with holes at the VBM while the higher peaks were associated with other $V-d$ t_{2g} orbitals, such as d_{xz} and d_{yz} . In a CL experiment electron hole pairs are first created by a high energy electron impact and then relax to the lowest states near the band edges before they radiatively recombine and emit light. So, first, it is not clear in this interpretation why the observed features are associated with density of states features in the conduction band only while ignoring the valence band structure and assuming that all holes have relaxed to the VBM. This would require one to assume a much faster hole than electron relaxation, for which there is no direct evidence, to the best of our knowledge. Second, the feature below 2 eV is about 0.5 below the absorption onset which was found to be near 2.35 eV by Kenny and Kannewurf[16]. Furthermore, adding Li would partially fill the split-off band and while one could imagine this to suppress absorption to these states, it would not really affect luminescent recombination between the split-off band and the VBM. The main observation of a decrease in the CL peak below 2 eV thus remains unexplained. Here we propose an alternative explanation.

First, luminescence and absorption are proportional to $\varepsilon_2(\omega)$ but in luminescence the lower energy region of the spectrum should be emphasized by the carrier relaxation toward the lowest electron and hole states. Furthermore, spontaneous luminescence is proportional to $R(\omega) \propto \omega^3 \varepsilon_2(\omega) / [e^{\hbar\omega/kT} - 1]$. Second, the optical absorption in pure V_2O_5 has recently been shown to be dominated by very strongly bound excitons [17, 18]. The first strong absorption occurs at 3 eV followed by peaks at 4 eV and 5-6 eV with the quasiparticle gap at 3.8 eV. We thus associate the CL peaks between 3-4 eV with the direct excitons. The absorption onset of V_2O_5 near 2.3-2.6 eV on the other hand is still not entirely understood but is likely associated with indirect excitons and/or a dark exciton becoming activated by phonons or disorder as discussed in [18, 38]. But while there can be a Stokes

shift between absorption and emission in localized state systems related to different structural relaxation in the ground and excited states, the CL feature at 1.8-1.9 eV is clearly not the same as the onset of absorption. We associate it with a polaronic emission or alternatively a self-trapped exciton. In fact, it has been shown by various calculations [20–22] that strong electron-phonon coupling leads to the formation of small electron polarons in V_2O_5 . The added electrons are usually associated with O-vacancies, in particular the vanadyl-O-vacancy. Scanlon *et al.* [20] showed that O-vacancies produce defect states at about 1 eV above the VBM similar to Li interstitials when a DFT+ U calculation is used which favors the formation of localized states and polaronic deformation. This was confirmed by Ngamwongwan *et al.* [21] and Watthaisong *et al.* [22] who showed that self-trapping of excitons occurs near an added electron even without the presence of O-vacancies or nearby Li interstitials. The self-trapped polaron is found near the middle of the gap at about 1 eV above the VBM, while the O-vacancy related states depend on which type of O is removed. We thus propose that the CL feature at 1.8-1.9 eV is associated with recombination of a self-trapped electron with holes at the VBM induced in the CL experiment. We can also view this as a self-trapped indirect exciton. It is not straightforward to extract the energy position of this band from the GGA+ U calculations of [20–22] as all of these miss the strong increase in quasiparticle gap we find in our QSGW calculations. However, we may assume that the polaron band lies close to the position of our Li induced band in LiV_2O_5 which is indeed about 2 eV above the VBM. While in our discussion above, this was associated with the spin splitting of the split-off band, the relaxation of the atoms near the Li which tilt the O-pyramids near each V toward the Li play also a decisive role in this feature being shifted down toward the middle of the gap. So, then why is this polaronic emission band reduced upon lithiation? At first one might think that the Li brings in more electrons and hence more polaron like states. However, there is now also a very strong absorption at about the same energy as the emission peak. We therefore propose that the emission is reduced by the strong absorption at this same energy. In other words, we propose that it is the phenomenon of self-reabsorption that reduces the cathodoluminescence at 1.8 eV.

V. CONCLUSIONS

In this paper we showed that Li electron donation in $\alpha\text{-LiV}_2\text{O}_5$ leads to a spin splitting of the split-off conduction band which creates an occupied band in the middle of the gap. This then leads to strong optical absorption between equal spin bands with intra-atomic $V-d$ character. Essentially transitions occur between antisymmetric and symmetric linear combinations of the d_{xy} orbitals on the two V across a V-O-V rung, which form strongly localized molecular type states. This strong absorption is

polarized exclusively along the a direction. We propose a different interpretation of the CL experiments of Walker *et al.* [4] with the main peaks at 3-4 eV being associated

with the charge transfer direct excitons of V_2O_5 and the 1.8 eV feature as an electron self-trapped polaron emission which is suppressed in LiV_2O_5 by self-absorption.

-
- [1] S. Sucharitakul, G. Ye, W. R. L. Lambrecht, C. Bhandari, A. Gross, R. He, H. Poelman, and X. P. A. Gao, V_2O_5 : A 2D van der Waals Oxide with Strong In-Plane Electrical and Optical Anisotropy, *ACS Applied Materials & Interfaces* **9**, 23949 (2017), pMID: 28677951.
- [2] M. S. Whittingham, The role of ternary phases in cathode reactions, *Journal of The Electrochemical Society* **123**, 315 (1976).
- [3] P. Y. Zavalij and M. S. Whittingham, Structural chemistry of vanadium oxides with open frameworks, *Acta Crystallographica Section B* **55**, 627 (1999).
- [4] M. J. Walker, A. Jarry, N. Pronin, J. Ballard, G. W. Rubloff, and L. J. Brillson, Nanoscale depth and lithiation dependence of v_2o_5 band structure by cathodoluminescence spectroscopy, *J. Mater. Chem. A* **8**, 11800 (2020).
- [5] A. Jarry, M. Walker, S. Theodoru, L. J. Brillson, and G. W. Rubloff, Elucidating Structural Transformations in $Li_xV_2O_5$ Electrochromic Thin Films by Multimodal Spectroscopies, *Chemistry of Materials* **32**, 7226 (2020).
- [6] Z. Levy, V. C. Ferrari, P. Rosas, M. J. Walker, K. Duddella, M. Haseman, D. Stewart, G. Rubloff, and L. J. Brillson, Lithium Spatial Distribution and Split-Off Electronic Bands at Nanoscale $V_2O_5/LiPON$ Interfaces, *ACS Applied Energy Materials* **6**, 4538 (2023).
- [7] Z. Warecki, V. C. Ferrari, D. A. Robinson, J. D. Sugar, J. Lee, A. V. Ievlev, N. S. Kim, D. M. Stewart, S. B. Lee, P. Albertus, G. Rubloff, and A. A. Talin, Simultaneous Solid Electrolyte Deposition and Cathode Lithiation for Thin Film Batteries and Lithium Iontronic Devices, *ACS Energy Letters* **9**, 2065 (2024).
- [8] E. I. Gillette, N. Kim, G. W. Rubloff, and S. B. Lee, Interconnected mesoporous V_2O_5 electrode: impact on lithium ion insertion rate, *Phys. Chem. Chem. Phys.* **18**, 30605 (2016).
- [9] X. Chen, E. Pomerantseva, K. Gregorczyk, R. Ghodssi, and G. Rubloff, Cathodic ALD V_2O_5 thin films for high-rate electrochemical energy storage, *RSC Adv.* **3**, 4294 (2013).
- [10] Y. Yue and H. Liang, Micro- and Nano-Structured Vanadium Pentoxide (V_2O_5) for Electrodes of Lithium-Ion Batteries, *Advanced Energy Materials* **7**, 1602545 (2017).
- [11] X. Rocquefelte, F. Boucher, P. Gressier, and G. Ouvrard, First-principle study of the intercalation process in the $Li_xV_2O_5$ system, *Chemistry of Materials* **15**, 1812 (2003).
- [12] V. Eyert and K.-H. Höck, Electronic structure of V_2O_5 : Role of octahedral deformations, *Phys. Rev. B* **57**, 12727 (1998).
- [13] L. R. De Jesus, G. A. Horrocks, Y. Liang, A. Parija, C. Jaye, L. Wangoh, J. Wang, D. A. Fischer, L. F. J. Piper, D. Prendergast, and S. Banerjee, Mapping polaronic states and lithiation gradients in individual V_2O_5 nanowires, *Nature Communications* **7**, 12022 (2016).
- [14] G. A. Horrocks, E. J. Braham, Y. Liang, L. R. De Jesus, J. Jude, J. M. Velázquez, D. Prendergast, and S. Banerjee, Vanadium K-Edge X-ray Absorption Spectroscopy as a Probe of the Heterogeneous Lithiation of V_2O_5 : First-Principles Modeling and Principal Component Analysis, *The Journal of Physical Chemistry C* **120**, 23922 (2016).
- [15] C. Bhandari, W. R. L. Lambrecht, and M. van Schilfgaarde, Quasiparticle self-consistent GW calculations of the electronic band structure of bulk and monolayer V_2O_5 , *Phys. Rev. B* **91**, 125116 (2015).
- [16] N. Kenny, C. Kannewurf, and D. Whitmore, Optical absorption coefficients of vanadium pentoxide single crystals, *Journal of Physics and Chemistry of Solids* **27**, 1237 (1966).
- [17] V. Gorelov, L. Reining, M. Feneberg, R. Goldhahn, A. Schleife, W. R. L. Lambrecht, and M. Gatti, Delocalization of dark and bright excitons in flat-band materials and the optical properties of V_2O_5 , *npj Computational Materials* **8**, 94 (2022).
- [18] C. Garcia, S. K. Radha, S. Acharya, and W. R. L. Lambrecht, Quasiparticle band structure and excitonic optical response in V_2O_5 bulk and monolayer, *Phys. Rev. B* **110**, 085102 (2024).
- [19] V. A. Ioffe and I. B. Patrino, Comparison of the Small-Polaron Theory with the Experimental Data of Current Transport in V_2O_5 , *Physica Status Solidi (b)* **40**, 389 (1970).
- [20] D. O. Scanlon, A. Walsh, B. J. Morgan, and G. W. Watson, An ab initio Study of Reduction of V_2O_5 through the Formation of Oxygen Vacancies and Li Intercalation, *The Journal of Physical Chemistry C* **112**, 9903 (2008).
- [21] L. Ngamwongwan, I. Fongkaew, S. Jungthawan, P. Hirunsit, S. Limpijumngong, and S. Suthirakun, Electronic and thermodynamic properties of native point defects in V_2O_5 : a first-principles study, *Phys. Chem. Chem. Phys.* **23**, 11374 (2021).
- [22] P. Watthaisong, S. Jungthawan, P. Hirunsit, and S. Suthirakun, Transport properties of electron small polarons in a V_2O_5 cathode of Li-ion batteries: a computational study, *RSC Adv.* **9**, 19483 (2019).
- [23] T. Kotani, M. van Schilfgaarde, and S. V. Faleev, Quasiparticle self-consistent GW method: A basis for the independent-particle approximation, *Phys. Rev. B* **76**, 165106 (2007).
- [24] B. Cunningham, M. Grüning, P. Azarhoosh, D. Pashov, and M. van Schilfgaarde, Effect of ladder diagrams on optical absorption spectra in a quasiparticle self-consistent GW framework, *Phys. Rev. Materials* **2**, 034603 (2018).
- [25] B. Cunningham, M. Grüning, D. Pashov, and M. van Schilfgaarde, QSGW: Quasiparticle self-consistent GW with ladder diagrams in W , *Phys. Rev. B* **108**, 165104 (2023).
- [26] D. Pashov, S. Acharya, W. R. Lambrecht, J. Jackson, K. D. Belashchenko, A. Chantis, F. Jamet, and M. van Schilfgaarde, Questaal: A package of electronic structure methods based on the linear muffin-tin orbital technique, *Computer Physics Communications*, 107065 (2019).
- [27] C. Bhandari and W. R. L. Lambrecht, Electronic and magnetic properties of electron-doped V_2O_5 and

- NaV₂O₅, Phys. Rev. B **92**, 125133 (2015).
- [28] C. Delmas, H. Cognac-Auradou, J. Cocciantelli, M. Ménétrier, and J. Doumerc, The Li_xV₂O₅ system: An overview of the structure modifications induced by the lithium intercalation, Solid State Ionics **69**, 257 (1994).
- [29] J. Galy, Vanadium pentoxide and vanadium oxide bronzes—Structural chemistry of single (S) and double (D) layer M_xV₂O₅ phases, Journal of Solid State Chemistry **100**, 229 (1992).
- [30] M. van Schilfgaarde, T. Kotani, and S. Faleev, Quasiparticle Self-Consistent *GW* Theory, Phys. Rev. Lett. **96**, 226402 (2006).
- [31] L. Hedin, New method for calculating the one-particle green's function with application to the electron-gas problem, Phys. Rev. **139**, A796 (1965).
- [32] L. Hedin and S. Lundqvist, Effects of electron-electron and electron-phonon interactions on the one-electron states of solids, in *Solid State Physics, Advanced in Research and Applications*, Vol. 23, edited by F. Seitz, D. Turnbull, and H. Ehrenreich (Academic Press, New York, 1969) pp. 1–181.
- [33] S. Ismail-Beigi, Justifying quasiparticle self-consistent schemes via gradient optimization in baym–kadanoff theory, Journal of Physics: Condensed Matter **29**, 385501 (2017).
- [34] F. Aryasetiawan and O. Gunnarsson, Product-basis method for calculating dielectric matrices, Phys. Rev. B **49**, 16214 (1994).
- [35] G. Onida, L. Reining, and A. Rubio, Electronic excitations: density-functional versus many-body Green's-function approaches, Rev. Mod. Phys. **74**, 601 (2002).
- [36] J. P. Perdew, K. Burke, and M. Ernzerhof, Generalized Gradient Approximation Made Simple, Phys. Rev. Lett. **77**, 3865 (1996).
- [37] S. Atzkern, M. Knupfer, M. S. Golden, J. Fink, A. N. Yaresko, V. N. Antonov, A. Hübsch, C. Waidacher, K. W. Becker, W. von der Linden, G. Obermeier, and S. Horn, One-dimensional dynamics of the d electrons in α' - NaV₂O₅, Phys. Rev. B **63**, 165113 (2001).
- [38] V. Gorelov, L. Reining, W. R. L. Lambrecht, and M. Gatti, Robustness of electronic screening effects in electron spectroscopies: Example of V₂O₅, Phys. Rev. B **107**, 075101 (2023).